

Solid state amorphization reactions in deformed Ni–Zr multilayered composites

G. C. Wong,^{a)} W. L. Johnson, and E. J. Cotts^{b)}

Keck Laboratory, California Institute of Technology, Pasadena, California 91125

(Received 17 July 1989; accepted 8 November 1989)

The mechanisms of metallic glass formation and competing crystallization processes in mechanically-deformed Ni–Zr multilayered composites have been investigated by means of differential scanning calorimetry and x-ray diffraction. Our investigation of the heat of formation of amorphous Ni_xZr_{1-x} alloys shows a large negative heat of mixing (on the order of 30 kJ/mole) for compositions near Zr₅₅Ni₄₅ with a compositional dependence qualitatively similar to that predicted by mean field theory. We find that the products of solid state reactions in composites of Ni and Zr can be better understood in terms of the equilibrium phase diagram and the thermal stability of liquid quenched metallic glasses. We have determined the composition of the growing amorphous phase at the Zr interface in these Ni–Zr diffusion couples to be $55 \pm 4\%$ Zr. We investigated the kinetics of solid state reactions competing with the solid state amorphization reaction and found the value of the activation energy of the initial crystallization and growth of the growing amorphous phase to be 2.0 ± 0.1 eV, establishing an upper limit on the thermal stability of the growing amorphous phase.

I. INTRODUCTION

Single phase amorphous alloys can form at relatively low temperatures (approximately half pertinent melting temperatures) by means of interdiffusion of pure, polycrystalline elements.¹⁻³ For instance, upon heating a multilayered, Ni/Zr diffusion couple at 600 K for 30 min, amorphous material (with a thickness of approximately 1000 Å) is observed to grow at the interfaces between the two metals. Thus a Ni/Zr composite with equal layer thicknesses of less than 1000 Å can be completely amorphized.⁴ Two requirements have been proposed for a successful solid state amorphization reaction, SSAR: (a) the two metals which form the diffusion couple must possess a large, negative heat of mixing in the amorphous phase and (b) there must be a dominant moving species; i.e., one constituent of the diffusion couple should exhibit a much greater mobility than the other.^{1,5,6} Such a disparity in the mobility of the atoms in the diffusion couple provides a constraint on the formation of equilibrium intermetallic compounds in a given temperature range and time frame, i.e., a kinetic constraint. The movement of both constituents is apparently required to nucleate and grow crystalline material while the mobility of only one constituent is required to grow an amorphous alloy.⁷

Experimental observations in the Ni/Zr system have been performed supporting both of these hypotheses. Various diffusion studies indicate that Ni is the dominant moving species in the SSAR in Ni/Zr diffusion couples.⁸⁻¹⁰ Differential scanning calorimetry (DSC) measurements have been utilized to establish that a negative difference in free energy between the pure elements and the amorphous phase (8–10 kcal/mol) drives these solid state amorphization reactions in the Ni/Zr system.^{4,11-13} In this present work we have studied solid state amorphization reactions in mechanically deformed Ni–Zr multilayered composites.^{12,14} The compositional dependence of the heat of mixing has been investigated and various aspects of the kinetic processes controlling these solid state amorphization reactions, including the competition between crystallization and amorphization processes, have also been studied. We find the thermal stability of the growing amorphous phase can be qualitatively understood in terms of the thermal stability of liquid quenched metallic glasses of similar stoichiometries.

II. EXPERIMENTAL PROCEDURE

Multilayered composites of transition and/or rare earth metals can be produced in bulk form relatively easily by means of mechanical deformation, thus facilitating a systematic study of solid state reactions. High purity (99.9%) foils of Zr and Ni metals were arranged in alternating layers, placed inside a stainless steel sheath (304 stainless with a number four finish), and

^{a)}Current address: Physics Department, University of California at Berkeley, Berkeley, California.

^{b)}Also with (and current address) The Department of Physics, Applied Physics and Astronomy, State University of New York at Binghamton, Binghamton, New York 13901.

then mechanically deformed in a rolling machine. The initial thickness of the composite was generally on the order of 50 microns. The composites were reduced in thickness by 50% to 67% by repeated passes through the rolling mill. A constant rolling direction was maintained within approximately 5 degrees. The deformation process was observed to cold weld the Zr and Ni foils together, with no apparent adhesion to the stainless steel sheath. The composite was removed from the deformed stainless steel sheath and the procedure was then repeated (with the deformed sample folded over on itself) a number of times, depending on the desired sample configuration (degree of deformation and the thickness of individual layers).

The foils utilized in this study were purchased commercially from several sources, or were obtained by cold rolling ingots. No effort was made to anneal or otherwise treat the foils; consistent results were observed in all aspects of the investigation regardless of the source of the foils. Foils and composites were routinely handled in air, with forceps or gloves. Composites were stored under vacuum.

The degree of deformation of a composite was characterized with the reduction ratio (RR):

$$RR = (i/f)^{2n} \quad (1)$$

with the initial thickness i and final thickness f of the composite, and n the number of times the composite is folded over on itself between runs. The reduction ratio provides a qualitative indication of the individual layer thicknesses and of the total interfacial area between individual layers, where ideally, for a given composite, individual layer thickness varies inversely with RR and the surface area is proportional to RR . In practice there is a distribution of layer thicknesses and RR is a qualitative indication of the composite configuration.^{12,14} Composites were characterized by means of x-ray diffraction analysis. A Norelco diffractometer with Ni-filtered, Cu K_α radiation was utilized in a standard θ - 2θ geometry.

Solid state reactions were monitored with a Perkin-Elmer DSC-4 differential scanning calorimeter (DSC) interfaced to an Apple IIE microcomputer. All samples for DSC scans were hermetically sealed in aluminum pans by cold welding the pans in an inert atmosphere. Reactions in diffusion couples were initiated as the samples were heated above room temperature in the DSC. The temperature of the sample was precisely controlled over long periods of time; i.e., a precise thermal history (within 0.1 K) could be imposed. The rate of heat release, dH/dt , was measured through the course of a reaction in order to quantify the kinetics controlling the amorphization process and subsequent processes. Integration of these data yields the enthalpy change, ΔH , associated with a phase or structural transformation of the sample. In the present study, the tempera-

ture of the DSC was varied at a constant rate. Standard procedure involved conducting DSC scans for a given thermal program with empty aluminum pans, in order to establish a baseline. Baseline scans were followed immediately by a number of scans (conducted under identical thermal conditions) with the encapsulated sample in place. Both the difference between the data from the second and third sample scans and difference between the second sample scan and the last baseline scan were examined to establish the precision of the measurement. A null difference (within experimental error) between the second and third sample scans ensured that any reaction was complete before the beginning of the second sample scan. Data from the second sample scan were subtracted from those of the first sample scan to obtain the rate of enthalpy release versus temperature associated with a given solid state reaction. No attempt was made to compensate for changes in the specific heat of the sample after the transformations undergone in the first sample scan.

III. RESULTS

The DSC scans¹¹ of different composites of average stoichiometry $\text{Ni}_{66}\text{Zr}_{34}$ shown in Fig. 1 reveal some basic features of solid state reactions in the Ni-Zr system. These scans were conducted at a constant scan rate of 10 K/min from 320 K to 870 K. X-ray diffraction analysis of numerous similar samples and samples of varying stoichiometries indicates that in general the broad exothermic DSC signal observed below 625 K is associated with the formation of amorphous material. Specifically, an x-ray diffraction (XRD) profile of a similar sample ($RR = 10^2$) heated at 10 K/min in the DSC to 625 K and quenched to room temperature reveals a broad peak

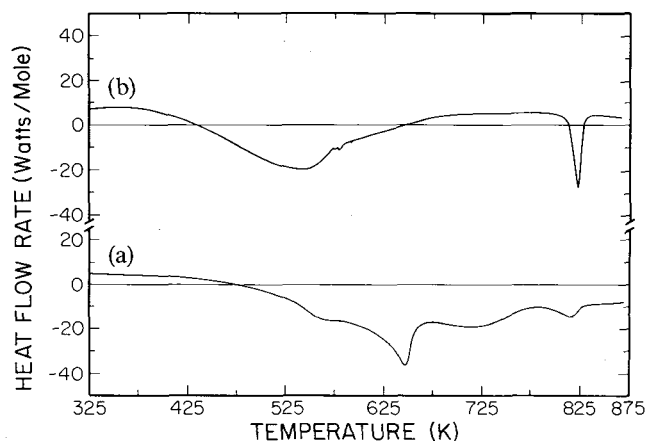


FIG. 1. The heat-flow rate as a function of temperature for a heating rate of 10 K/min, measured by means of differential scanning calorimetry. The samples were multilayered composites of Zr and Ni of average stoichiometry $\text{Ni}_{66}\text{Zr}_{34}$, produced by means of co-deformation of the two metals. (a) A sample of reduction ratio of 10^2 . (b) A sample of reduction ratio of 10^4 .

centered at $2\theta \approx 40$ deg, corresponding to an XRD profile of liquid quenched, amorphous material of a composition near $\text{Ni}_{60}\text{Zr}_{40}$. Examination of Ni-Zr composites of various compositions and reduction ratios reveals a correlation between the sharp exothermic peak at 650 K in DSC scans taken at 10 K/min and the appearance of Bragg peaks in the corresponding XRD profile associated with orthorhombic $\text{Ni}_{50}\text{Zr}_{50}$. For example, the XRD profile of a sample similar to that of Fig. 1(a) heated at 10 K/min in the DSC to a temperature of 675 K and quenched to room temperature indicates that in addition to amorphous material, the intermetallic orthorhombic compound, $\text{Ni}_{50}\text{Zr}_{50}$, has been formed. Such a DSC peak generally signals the end of the solid state amorphization reaction; subsequent solid state reaction results in the formation and/or growth of crystalline compounds. In contrast, the DSC scan of Fig. 1(b) is for a sample of a relatively high reduction ratio, i.e., a sample with thin (<1000 Å) layers. In Fig. 1(b) the solid state amorphization reaction continues essentially to completion and any peaks observed in the DSC trace at higher temperatures correspond simply to the crystallization of amorphous material of stoichiometry close to that of the composite.

Due to the nature of the mechanical deformation process, some information on the geometry of a given composite is lost. Rather than multilayers of Ni and Zr of uniform individual layer thicknesses (as generally obtained by means of thin film deposition¹⁵), scanning electron microscope studies indicate that mechanically deformed composites display a distribution of layer thicknesses.^{12,14} This difference in the distribution of layer thicknesses is reflected in DSC scans; in fact, comparison of composites produced by means of mechanical deformation and by thin film deposition provides a qualitative illustration of the distribution of layer thicknesses in the mechanically deformed sample.

We observe a significant difference between the DSC thermograms of Ni-Zr composites with an average stoichiometry of $\text{Ni}_{58}\text{Zr}_{42}$ produced by sputtering as compared to those produced by means of mechanical deformation. In Fig. 2, DSC scans are presented for multilayered composites produced by means of sputtering (from a previous work¹⁶), with Zr metal layer thicknesses of 800, 450, and 240 Å in Figs. 2(a), 2(b), and 2(c), respectively, and a mechanically deformed sample in Fig. 2(d). In the sputtered composites, the temperature at which the maximum heat release occurs varies monotonically with layer thickness. Assuming a smooth distribution of layer thicknesses, the average single layer thickness in the mechanically deformed sample is expected to correspond roughly to the thickness of individual layers in the sputtered sample which exhibits the same peak temperature in DSC scans of the glass-forming reaction as the mechanically deformed sample itself. Moreover, the initial large exothermic signal

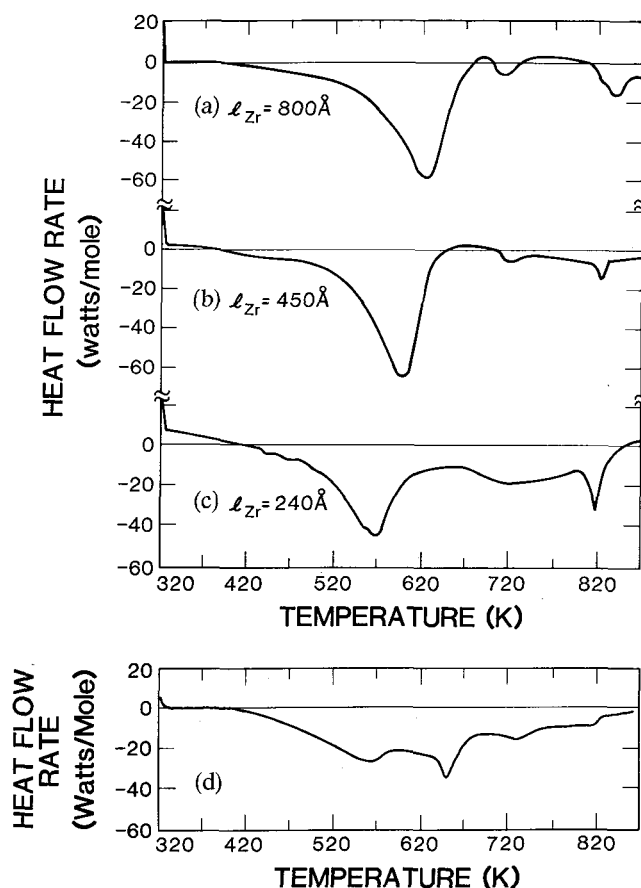


FIG. 2. The heat-flow rate as a function of temperature for a heating rate of 10 K/min, measured by means of differential scanning calorimetry. The samples were multilayered composites of Zr and Ni of average stoichiometry $\text{Ni}_{58}\text{Zr}_{42}$. The data in curves (a)–(c) are from Ref. 16 and correspond to samples produced by means of atomic deposition by sputtering while the data in curve (d) correspond to a sample produced by means of codeformation of the two metals. (a) A sputtered sample with Zr layers of thickness of 800 Å. (b) A sputtered sample with Zr layers of thickness of 450 Å. (c) A sputtered sample with Zr layers of thickness of 240 Å. (d) A mechanically-deformed sample with a reduction ratio 5000.

corresponding to the glass-forming reaction is approximately twice as broad for the mechanically deformed samples than for the sputtered Ni/Zr multilayers. Data from DSC scans for sputtered multilayered samples of varying thicknesses can be scaled and superposed to duplicate the DSC data corresponding to the mechanically deformed sample, providing a qualitative estimate of the width of the distribution of layer thicknesses in the mechanically deformed sample. Our data indicate that the average single layer thickness in the mechanically deformed sample is on the order of 100 Å, whereas a calculation of the single layer thicknesses assuming uniform reduction without slippage during the deformation process would suggest a value of 5 Å. This qualitative analysis also suggests there are a significant number of layers with thicknesses near 1000 Å. Our observations made by

means of DSC are consistent with direct observations made by means of scanning electron microscopy.¹⁴

It is to be noted that the initial stages (e.g., Fig. 2) of the reactions are generally qualitatively similar for samples produced both by thin film deposition and by mechanical co-deformation. Generally a reaction begins at approximately 420 K and the rate increases with increasing temperature in a monotonic manner. It has been previously indicated that a degree of disorder is required at the interface in order for the amorphous phase to grow at these temperatures and times⁷ (and that this amount of disorder is present in Ni/Zr multilayers produced by sputtering). The larger degree of disorder which is presumably present at the interface of the highly deformed composites does not seem to alter dramatically the initial stages of these solid state reactions in the Ni-Zr system. In systems different from Ni-Zr, where composites prepared by thin film deposition have a relatively large degree of order at interfaces, differences in solid state reactions may be observed between samples prepared by these two methods. That is, in other systems the expected large degree of disorder present at interfaces of mechanically deformed composites may result in significant differences in reaction kinetics.

These solid-state amorphization reactions are driven by a large negative heat of mixing. Previously we directly measured the heat of formation of amorphous $Zr_{32}Ni_{68}$ alloy from the elemental metals and found it to be 35 ± 5 kJ/mole.⁴ This measurement was performed by monitoring a solid state amorphization reaction by means of DSC. The rate of heat flow, dH/dt , as measured for a constant heating rate was integrated from temperatures of 370 K to 720 K. In the present study we have examined the compositional dependence of the heat of mixing of amorphous alloys in the Ni-Zr system, utilizing a more indirect method. Mechanically deformed composites of a known average stoichiometry were heated at a constant rate from a temperature of 320 K to 870 K (Fig. 3). Integration of these data provided the total enthalpy release, ΔH , corresponding to any transformations which the composite underwent. X-ray analysis was utilized to examine the product of the ensuing reactions. In general, the equilibrium phase was found to have formed, with a small amount (less than 5%) of the composite remaining unreacted. Thus the measured ΔH corresponds to a measurement (with a relatively large error on the order of 10%) of the heat of formation of the intermetallic compounds (or phase mixture of intermetallic compounds, as predicted by the equilibrium phase diagram) at a given stoichiometry in the Ni-Zr system. The heats of crystallization (i.e., the enthalpy release upon transformation from the amorphous state to a crystalline phase) have been previously determined for a range of stoichiometries of amorphous alloys in the Zr-Ni system (generally measuring from 4 to 6 kJ/mole).^{17,18} For a particular stoi-

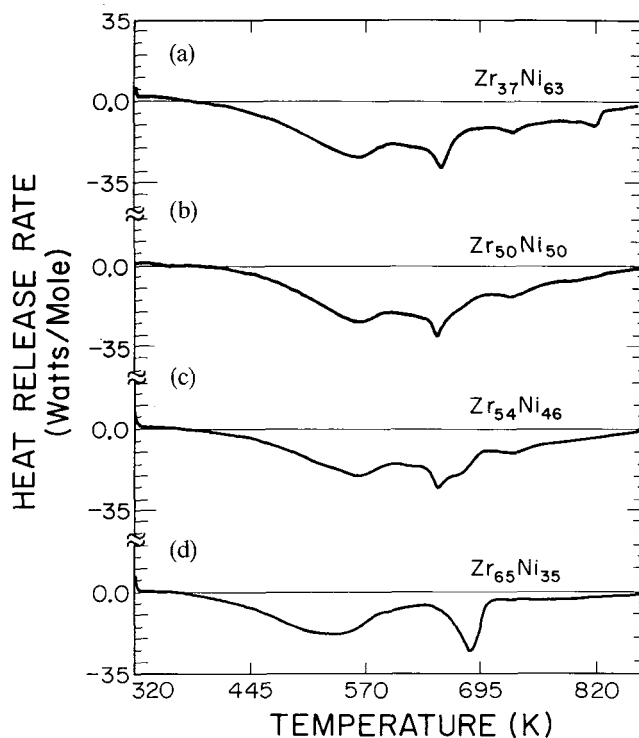


FIG. 3. The heat-flow rate as a function of temperature for a heating rate of 10 K/min, measured by means of differential scanning calorimetry. The samples were multilayered composites of Zr and Ni of varying average stoichiometries (as noted in the figure), produced by means of codeformation of the two metals. All samples were of high reduction ratio, on the order of 50 000.

chiometry, we subtract the heat of crystallization as reported in the literature from the heat of formation of the equilibrium phase which we have measured, to yield an estimate of the heat of formation of the amorphous phase.^{19,20} The experimental results are presented in Fig. 4, along with a calculation of the heat of formation of the amorphous phase due to Saunders and Miodownik.²¹ The data for the heat of formation of the amorphous phase show a composition dependence which is in qualitative agreement with mean field theory calculations.^{20,21} The magnitude of the heat of formation observed is, even upon accounting for experimental error, less than that observed by means of a solution calorimeter.²²

Except at short times, the growth of amorphous material by means of solid state reaction in the Ni-Zr system is diffusion limited.^{23,24} Thus a composition gradient exists in the growing amorphous phase, with the composition at the endpoints fixed. Analysis of data obtained previously by means of Rutherford backscattering indicated that the endpoint compositions are $Zr_{54}Ni_{46}$ at the Zr interface and $Zr_{32}Ni_{68}$ at the Ni interface.²⁵ By means of x-ray analysis we investigate the composition at the Zr interface.

Zr-rich composites of high reduction ratio were annealed for long times at temperatures such that the

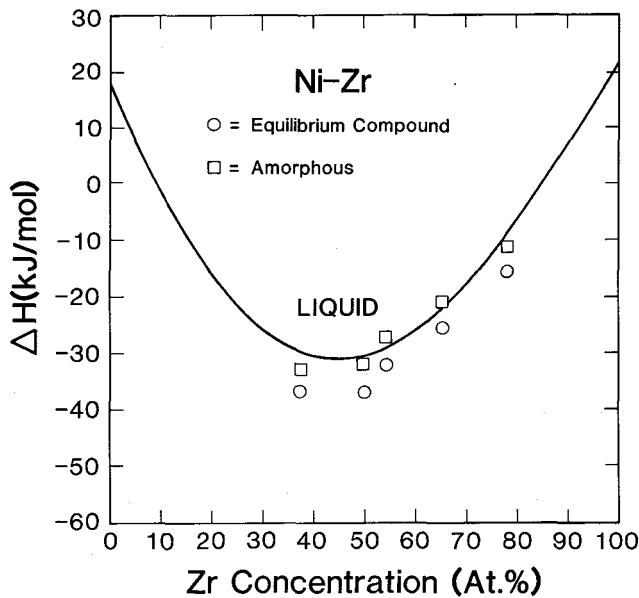


FIG. 4. Enthalpy of formation versus composition. ○: The integrated enthalpy release for the heat-flow as measured by means of differential scanning calorimetry. The samples were multilayered composites of Zr and Ni, produced by means of codeformation of the two metals. All samples were of high reduction ratio, on the order of 50000. ●: The calculated enthalpy of formation of the amorphous phase. Measured heats of crystallization were subtracted from measured enthalpies of formation of the equilibrium crystalline phases. The line corresponds to a calculation by Saunders and Miodownik.²¹

solid state amorphization reaction was completed but no equilibrium compounds were formed.⁹ The proper metastable phase diagram including pure Ni and Zr metals and amorphous Zr-Ni alloys would indicate that after such an anneal only Zr metal and an amorphous alloy at the composition endpoint should exist. At a Zr-rich stoichiometry such as $Zr_{78}Ni_{22}$ and a high RR ratio we expect the thickness of the majority of the individual Ni layers to be less than 100 Å, with only a small percentage thicker than 300 Å. Previous observation has shown that composites of Ni-rich stoichiometries with similar or thinner individual Ni layers are completely amorphized under similar heat treatments.^{4,9,26} For instance, a multilayered sample produced by means of sputtering with 300 Å individual layer thicknesses is amorphized upon heating at 10 K/min to 655 K. Thus upon heating our composites we expect rapid depletion of elemental Ni. Ni atoms should continue to diffuse out of the amorphous phase into the Zr metal, as the growth of amorphous material continues, thereby homogenizing the amorphous layer until the equilibrium composition of the amorphous phase at the Zr interface is reached. A schematic drawing of the steps of these solid state reactions is presented in Fig. 5. The common tangent rule applied to a free energy diagram of the amorphous phase and elemental Zr suggests that the

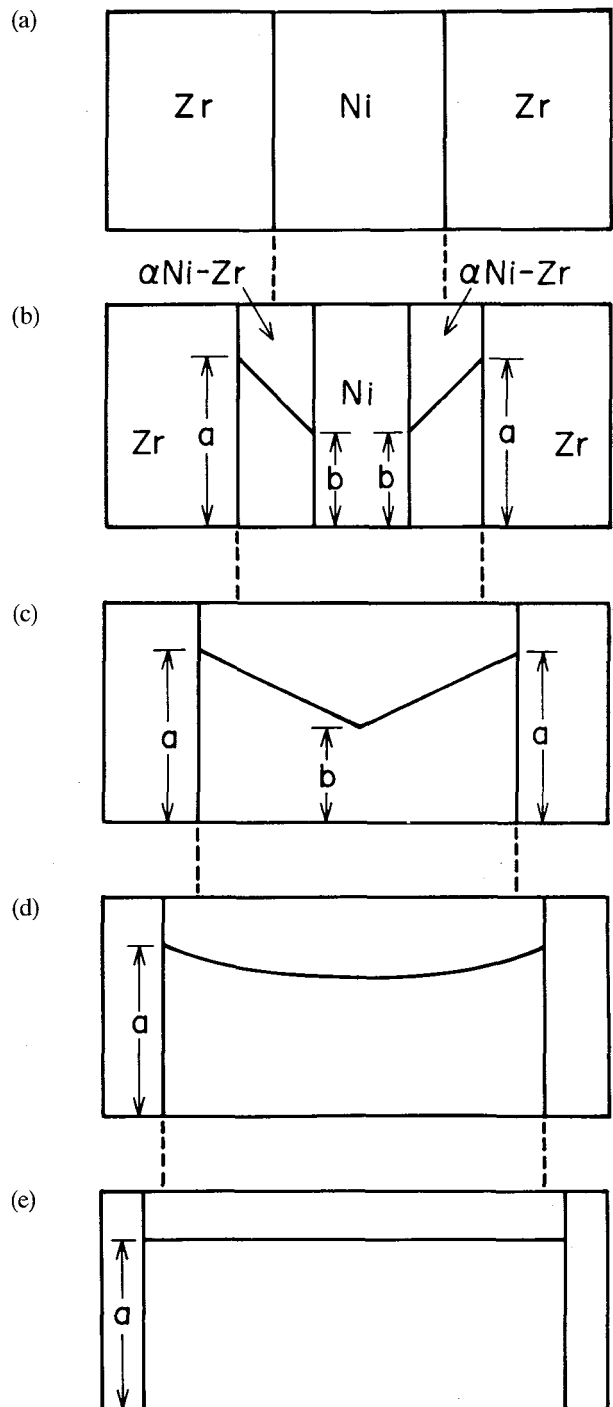


FIG. 5. A schematic illustration of a solid state amorphization reaction in the Zr-Ni system in a Zr-rich diffusion couple. The Zr concentration is plotted versus length in the amorphous interlayers between pure Zr and pure Ni metal. (a) The Zr-Ni diffusion couple as-prepared. (b) The growth of an amorphous interlayer at each interface is illustrated, assuming a linear concentration gradient. The compositions at the endpoints of the profile are indicated by the letter "b" at the Ni interface and the letter "a" at the Zr interface. (c) A sketch of the instant when the Ni metal is depleted everywhere on the interface. (d) The homogenization of the diffusion couple after the Ni metal has been depleted. (e) A fully homogenized amorphous interlayer, with Zr metal and amorphous alloy.

driving force for the reaction decreases as the homogenization progresses, but with our relatively short diffusion distances we would expect to maximize the homogeneity of the amorphous phase. In the case of incomplete homogenization, the average composition of the amorphous layer formed constitutes a lower bound on the Zr content of the Zr-interface composition.

The determination of the composition endpoint depended on the ability to determine the stoichiometry of amorphous material by means of x-ray diffraction. It has previously been observed that amorphous Zr_xNi_{1-x} alloys ($0.2 < x < 0.7$) all exhibit similar x-ray diffraction profiles indicative of the amorphous phase with the position of the broad, primary XRD peak varying monotonically with composition x . We utilized the extensive data from the literature along with similar data routinely gathered in our laboratory.^{18,26} In our analysis the parameter

$$d = \frac{1.5418}{2 \sin \theta}, \quad (2)$$

where θ corresponds to the angle of the maximum of the first, broad peak in x-ray scans was plotted versus concentration x and this function was fit with a two-dimensional polynomial, for Ni concentrations $x = 0.2$ to $x = 0.7$. The fitting function can be utilized to estimate from its x-ray diffraction profile the stoichiometry of an amorphous alloy of composition Zr_xNi_{1-x} with concentration x between 0.2 and 0.7.

In order to estimate the composition at the amorphous layer/Zr metal interface, composite samples of average stoichiometry $Zr_{78}Ni_{22}$ with $RR = 6 \times 10^4$ or $Zr_{65}Ni_{35}$ with $RR \approx 10^4$ were heated from 320 K to 635 K in the DSC at 10 K/min, and then quenched to room temperature for x-ray analysis. Examination of the x-ray diffraction profile of the $Zr_{65}Ni_{35}$ composite after this heat treatment reveals that the Bragg peaks corresponding to elemental Ni have essentially vanished, while a broad peak centered at $2\theta = 38$ deg corresponding to amorphous material of average stoichiometry near $Zr_{55}Ni_{45}$ has appeared. A significant amount of elemental Zr remains, as evidenced by the Bragg peaks near $2\theta \sim 36$ deg (Fig. 6). The amorphous material formed in both the Zr-rich composites ($Zr_{78}Ni_{22}$ and $Zr_{65}Ni_{35}$) is estimated to have a composition of approximately $Zr_{55}Ni_{45}$, with an estimated error of 4% in the determination of the stoichiometry. The source of this error is the inherent difficulty in deconvoluting the Bragg peak at $2\theta = 36.5$ deg [Zr(101)] from the broad peak corresponding to the amorphous phase. This estimate of the composition of the amorphous phase at the Zr-rich boundary of the diffusion couple does agree within experimental error with the previous estimate, $Zr_{53}Ni_{47}$, based upon analysis of Rutherford backscattering data.²⁵

The effects of layer thickness on solid state amorphization reactions in Ni-Zr multilayer composites

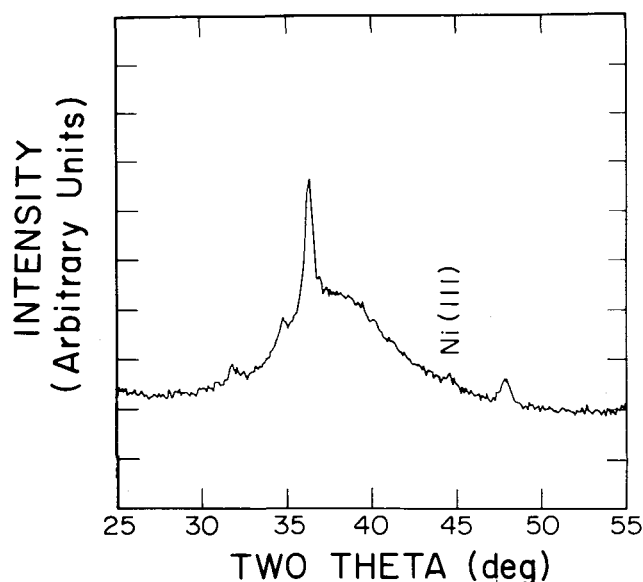


FIG. 6. X-ray diffraction profile (Cu K_α radiation) for a mechanically deformed Zr-Ni composites of average stoichiometry $Zr_{65}Ni_{35}$ which had been heated from 320 K to 635 K at a rate of 10 K/min and cooled rapidly to room temperature.

were investigated. A composite was mechanically deformed in the rolling mill and samples were removed from the composite at various stages of deformation for study. A series of DSC thermograms of samples (all of average stoichiometry $Zr_{78}Ni_{22}$) mechanically deformed to various degrees (reduction ratios from 130 to 57000) are displayed in Fig. 7. Upon heating samples similar to those utilized to produce the data in Fig. 7 to temperatures below 600 K, quenching to 320 K, and performing x-ray analysis, a broad peak associated with amorphous material along with sharp Bragg peaks associated with unreacted Ni and Zr are observed. Repeating this procedure with heating to temperatures above 600 K generally results in the observation of additional Bragg peaks associated with intermetallic compounds. Both DSC and x-ray diffraction data indicate that as the sample is deformed and the average layer thickness decreases, a larger fraction of the sample reacts at temperatures below 600 K. That is, more amorphous material is formed in DSC scans at 10 K/min. Such an observation supports the previous contention that layer thickness is a dominant parameter in determining the efficiency of a solid state amorphization reaction in the Ni-Zr system.

The data of Fig. 7 indicate that upon heating a Ni-Zr diffusion couple with layers of thickness greater than about 1000 Å, the intermetallic compound $Ni_{50}Zr_{50}$ is formed, followed by the formation of Zr_2Ni at higher temperature. Previous study has shown that the crystallization temperatures of liquid quenched metallic glasses in the Ni-Zr system decrease monotonically with increasing Zr content in the stoichiometric range in question. Therefore the most Zr-rich amorphous material in the

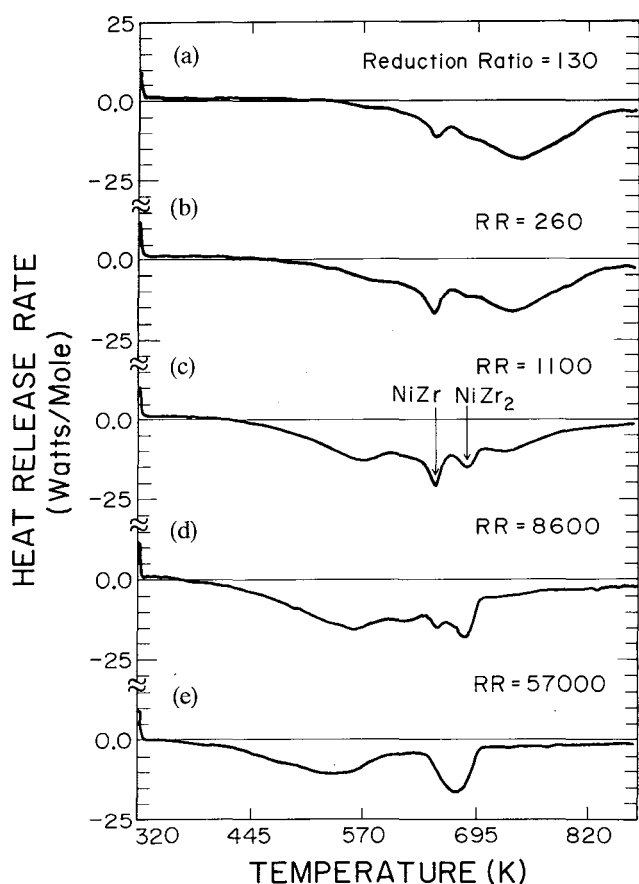


FIG. 7. The heat-flow rate as a function of temperature for mechanically deformed multilayered composites of Ni and Zr, as measured by means of differential scanning calorimetry. The samples are all of average stoichiometry $Zr_{78}Ni_{22}$. All differential scanning calorimetry scans are at a constant heating rate. The samples are of various degrees of deformation, as reflected in the differing reduction ratios, RR , with $RR = 57000$ corresponding to the most deformed sample. Exothermic peaks which have been correlated with the formation of particular crystalline compounds are indicated for the data depicted in (c).

growing diffusion couple, which is in fact in contact with crystalline Zr, would be expected to be the least thermally stable. The growth of orthorhombic $Ni_{50}Zr_{50}$ at the Zr interface in a diffusion couple has in fact been previously observed by means of transmission electron microscopy in the Ni-Zr system (in multilayered composites produced by means of thin film deposition). By scanning similar samples in different DSC runs at 10 K/min to various high temperatures corresponding to the various features of the observed peaks, quenching to room temperature and performing structural analysis by means of x-ray diffractometry the peaks observed at temperatures >600 K in the DSC scans in Fig. 7 can be correlated with structural changes in the sample. X-ray diffraction data indicate that the first peak (at a temperature of ~ 650 K) in the DSC thermograms Figs. 7(a)–7(d) corresponds to the formation of $Ni_{50}Zr_{50}$, while the sec-

ond peak (at a temperature of ~ 685 K) corresponds to the formation of $NiZr_2$. This is evidenced by the x-ray diffraction profiles of Figs. 8(a)–8(c), which reveal the presence of the above-mentioned intermetallic compounds only after the sample has been heated to temperatures at which the associated DSC peak has been observed. It is noted that the crystalline phases formed tend to be textured. These particular data which correlate certain DSC peaks with the nucleation and growth of specific crystalline phases are representative of those gathered at different quench temperatures, as well as for different stoichiometries and reduction ratios in the Ni-Zr system.

At increasing reduction ratios of composites of average stoichiometry $Zr_{78}Ni_{22}$, DSC scans of the composites reveal that the DSC peaks corresponding to the formation of $Ni_{50}Zr_{50}$ and $NiZr_2$ begin to overlap and at a $RR \sim 60000$ are indistinct. This observation apparently reflects a change only in the kinetics of nucleation and growth of the crystalline phases; the solid state amorphization reaction remains dominant at temperatures below 600 K in DSC scans at 10 K/min for all RR 's. The phase diagram for the Ni-Zr system indicates that at a composition of $Zr_{78}Ni_{22}$, crystalline Zr and the equilibrium compound Zr_2Ni should coexist. The fact that the equilibrium compound $Zr_{50}Ni_{50}$ forms first in this solid state reaction reflects the fact that the composition of the amorphous material at the interface between the growing amorphous Ni-Zr material and the crystalline Zr is close to $Zr_{50}Ni_{50}$, as well as possible differences in the kinetics of the formation of these two compounds. The nucleation and growth of $NiZr_2$ in equilibrium concentrations require a transformation of the existent $Ni_{50}Zr_{50}$ compound as well as diffusion of Ni atoms into crystalline Zr. As the average layer thickness decreases with increasing RR , the diffusion distance required to form Zr_2Ni decreases and at a given temperature this equilibrium compound forms more rapidly. The DSC peak associated with the nucleation and growth of Zr_2Ni increases in magnitude with increasing reduction ratio (i.e., with decreasing layer thickness) until the peak associated with $Ni_{50}Zr_{50}$ nucleation and growth is no longer distinguishable [Fig. 7(e)].

Upon heating these Ni-Zr composites at a constant rate from room temperature to high temperatures a solid state amorphization reaction ensues, followed by—depending on the thickness of the layers—the nucleation and growth of certain crystalline compounds. Unless the Zr metal is consumed at low temperature, orthorhombic $Zr_{50}Ni_{50}$ is the first intermetallic compound to form from the amorphous phase, forming at the Zr interface. This observation is supported by a large amount of data, including the DSC scans of Fig. 7 at various scan rates for a composite of average stoichiometry $Zr_{58}Ni_{42}$ and for the DSC scans of Fig. 3 of 10 K/min for composites of various stoichiometries. For thin layered composites

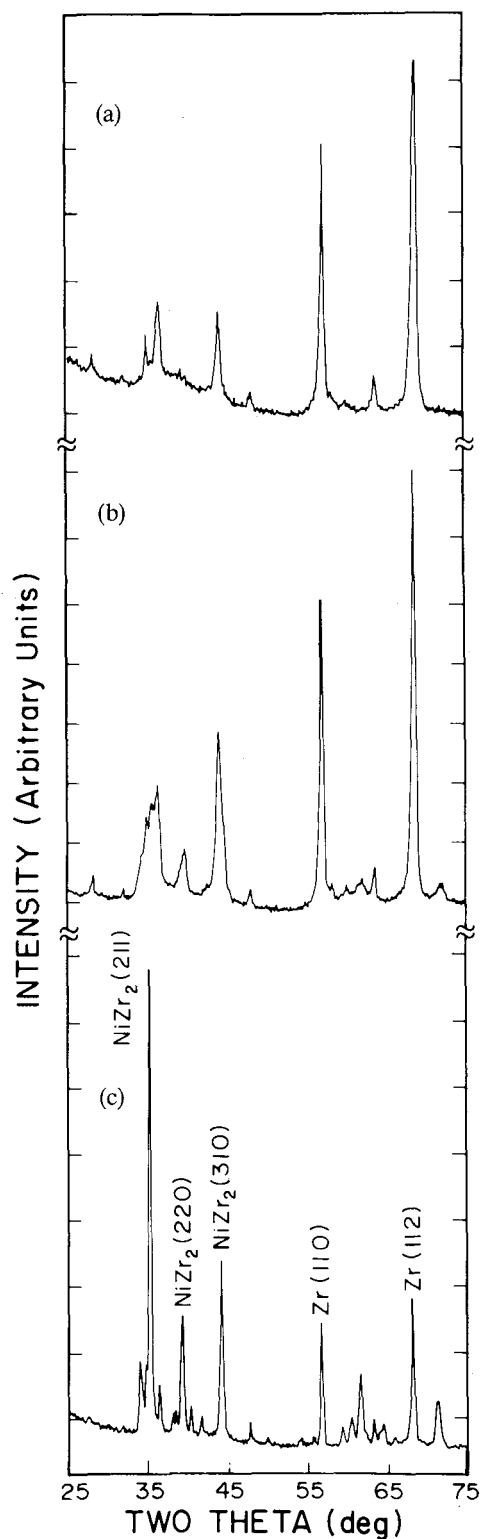


FIG. 8. X-ray diffraction profiles (Cu K_{α} radiation) for mechanically deformed Zr-Ni composites of average stoichiometry $Zr_{78}Ni_{22}$ which had been heated from 320 K to various temperatures at a rate of 10 K/min and cooled rapidly to room temperature. (a) X-ray diffraction profile after heating to 665 K. (b) X-ray diffraction profile after heating to 695 K. (c) X-ray diffraction profile after heating to 870 K.

(layer thicknesses $< 1000 \text{ \AA}$) the product of the solid state reaction reflects the relative abundance of crystalline Ni and crystalline Zr. That is to say, either the Ni or the Zr metal is consumed at a relatively low temperature. Intermetallic compounds of stoichiometries rich in a metal which has been consumed are less likely to form at the expense of a compound closer to the overall stoichiometry of the composite. For the Ni-rich composite in Fig. 3(a) and the composite of stoichiometry $Ni_{50}Zr_{50}$ in Fig. 3(b), the DSC peaks observed at higher temperatures correspond to the formation of Ni-rich compounds. The equilibrium phase diagram is relatively complicated in this composition region, with numerous compounds observed. The distinct DSC peak in Fig. 3(a) observed near 820 K corresponds to the singular crystallization peak in DSC scans of liquid-quenched amorphous $Zr_{32}Ni_{68}$. X-ray diffraction analysis of both liquid quenched metallic glass and mechanically deformed composites of similar stoichiometries which were heated to 870 K at 10 K/min and quenched to room temperatures resulted in similar diffraction profiles. The products of solid state reactions in composites of Ni and Zr can be better understood in terms of the thermal stability of liquid quenched metallic glasses and the equilibrium phase diagram.

The kinetics of the initial formation of crystalline material in the growing diffusion couple (i.e., of the nucleation and growth of orthorhombic $Zr_{50}Ni_{50}$) have been examined.⁹ The temperature of the formation of orthorhombic $Zr_{50}Ni_{50}$, T_c , was evaluated as a function of DSC scan rate, s . The values of T_c were determined from the maximum of exothermic DSC peaks which had been correlated with the formation of orthorhombic $Zr_{50}Ni_{50}$ by means of x-ray diffraction analysis for a series of DSC scans of heating rates varying from 0.2 to 200 K/min (Fig. 9). In order to determine the activation energy, E_c , for the initial formation and growth of orthorhombic $Zr_{50}Ni_{50}$, these data are plotted in Fig. 10 in the form $\ln [s/T_c^2]$ vs $1/T_c$, as dictated by Kissinger's method.²⁸ In this Kissinger analysis, the slope of this plot is proportional to $-E_c/R$, where R is the gas constant. A simple least squares fit to the data is performed. Thus we determine the activation energy of this crystallization process to be $E_c = 2.0 \pm 0.1 \text{ eV/atom}$.

The observed value of E_c is significantly higher than the activation energy, E_a , for interdiffusion of Ni and Zr atoms in the early or middle stages of the growing amorphous phase⁴ ($E_a = 1.1 \pm 0.1 \text{ eV}$). The observed value of E_c is less than the reported activation energy, E_x , for crystallization of liquid-quenched metallic glass of composition close to $Zr_{54}Ni_{46}$, the composition at the interface between the growing amorphous phase and the Zr metal, $E_x = 3.5 \text{ eV}$ for liquid quenched $Zr_{55}Ni_{45}$ (activation energies of 2.4 eV and 2.9 eV have

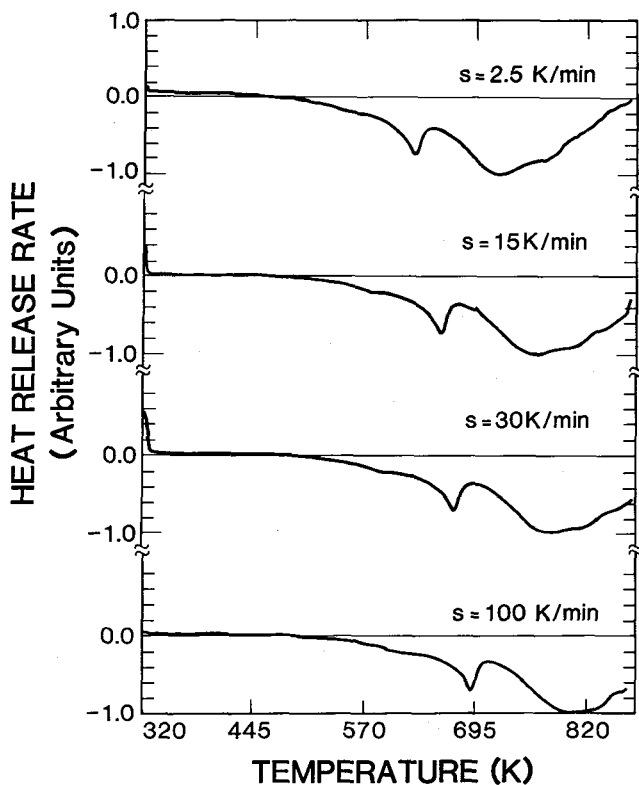


FIG. 9. The heat-flow rate as a function of temperature for mechanically deformed multilayered composites of Ni and Zr, as measured by means of differential scanning calorimetry. The samples are all of average stoichiometry $Zr_{42}Ni_{58}$. The heating rate, s , for each differential scanning calorimetry scan is indicated in the figure.

been reported for liquid quenched metallic glasses of stoichiometry $Zr_{50}Ni_{50}$ and $Zr_{48}Ni_{52}$, respectively^{17,18}). The data which we have obtained for the slowest DSC scan rates (0.2–2.5 K/min) overlap the kinetic region (time and temperature) of previous isothermal annealing experiments which utilized transmission electron microscopy to characterize structural changes.²⁹ Previous study has shown that in this kinetic region orthorhombic $Zr_{50}Ni_{50}$ grew at the interface between the amorphous phase and the Zr metal and that the growth was into the Zr metal, with only limited consumption of the amorphous phase.^{29,30} These observations are consistent with nucleation and growth of orthorhombic $Zr_{50}Ni_{50}$ at the Zr interface of the diffusion couple. The value of the activation energy, E_c , may reflect a heterogeneous crystallization process involving some rearrangement of Zr atoms. This would explain why E_c is less than E_x , as the crystallization of liquid quenched metallic glass may be closer to a homogeneous process. The fact that E_c is greater than E_a probably reflects the fact that the interdiffusion involved in the solid state amorphization reaction is dominated by the move-

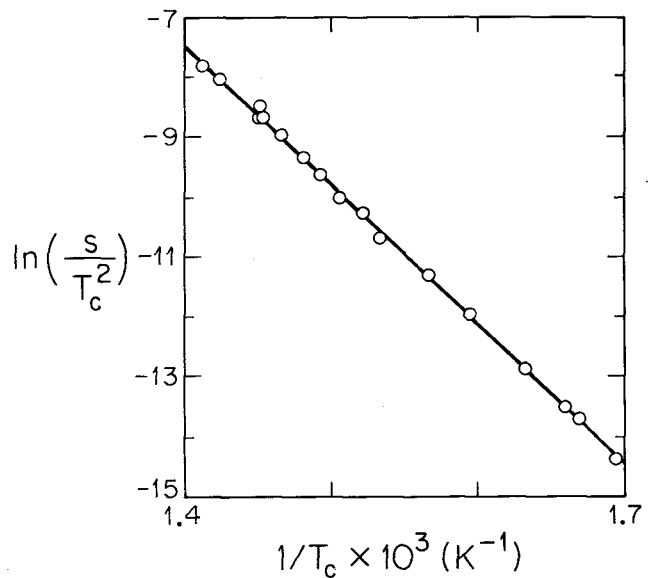


FIG. 10. The natural logarithm of the heating rate, s , divided by the square of the crystallization temperature, T_c , versus the inverse crystallization temperature. The solid line is a least squares fit to the data.

ment of Ni atoms while the formation of orthorhombic $Zr_{50}Ni_{50}$ requires some movement of Zr atoms at a higher activation energy. The thermal stability of the amorphous phase at the Zr interface determines an upper limit on the thermal stability of the amorphous Zr/Ni diffusion couple.

IV. CONCLUSIONS

We have found that multilayered composites of transition metals can be produced in bulk form relatively easily by means of mechanical deformation, thus facilitating a study of solid state amorphization reactions in the Ni–Zr system. Our investigation of the heat of formation of amorphous Ni_xZr_{1-x} alloys shows a large negative heat of mixing (on the order of 8–10 kcal/mole) for compositions near $Zr_{55}Ni_{45}$ with a compositional dependence qualitatively similar to that predicted by mean field theory. We find that the products of solid state reactions in composites of Ni and Zr can be better understood in terms of the equilibrium phase diagram and the thermal stability of liquid quenched metallic glasses. We have determined the composition of the growing amorphous phase at the Zr interface in these Ni–Zr diffusion couples to be $55 \pm 4\%$ Zr. We investigated the kinetics of solid state reactions competing with the solid state amorphization reaction and found the value of the activation energy of the initial crystallization and growth of the growing amorphous phase to be 2.0 ± 0.1 eV, establishing an upper limit on the thermal stability of the growing amorphous phase.

ACKNOWLEDGMENTS

We thank M. Atzmon, W. J. Meng, and K. Samwer for helpful discussions. This work was supported by the United States Department of Energy Contract No. DE-AT03-81ER10870, while one author, E. Cotts, was supported in the later stages of this work by the Research Corporation Grant C-2587.

REFERENCES

- ¹R. B. Schwarz and W. L. Johnson, *Phys. Rev. Lett.* **51**, 415 (1983).
- ²W. L. Johnson, *Prog. Mater. Sci.* **30**, 80 (1986).
- ³*Proc. of the Conf. on Solid State Amorphizing Transformations*, edited by R. B. Schwarz and W. L. Johnson, *J. Less-Common Met.* **140**, 335 (1988).
- ⁴E. J. Cotts, W. J. Meng, and W. L. Johnson, *Phys. Rev. Lett.* **57**, 2295 (1986).
- ⁵K. Samwer, *Phys. Rep.* **161**, 1 (1988).
- ⁶L. Schultz and E. Hellstern, in *Science and Technology of Rapidly Quenched Alloys*, edited by M. Tenhover, W. L. Johnson, and L. E. Tanner, Materials Research Society Symposia Proceedings (Materials Research Society, Pittsburgh, PA, 1987), Vol. 80 and other papers in this volume.
- ⁷A. M. Vredenberg, J. F. M. Westendorp, F. W. Saris, N. M. van der Pers, and Th. H. de Keijser, *J. Mater. Sci.* **1**, 774 (1986).
- ⁸Y. T. Cheng, W. L. Johnson, and M. A. Nicolet, *Appl. Phys. Lett.* **47**, 800 (1985).
- ⁹H. Hahn, R. S. Averback, and S. J. Rothman, *Phys. Rev. B* **33**, 8825 (1986).
- ¹⁰H. Hahn and R. S. Averback, *Phys. Rev. B* **37**, 6537 (1988).
- ¹¹E. J. Cotts, G. C. Wong, and W. L. Johnson, *Phys. Rev. B* **37**, 9049 (1988).
- ¹²L. Schultz, in *Rapidly Quenched Metals*, edited by S. Steeb and H. Warlimont (North-Holland, Amsterdam, 1984), p. 551; L. Schultz, in *Proc. of the 6th Int. Conf. on Liquid and Amorphous Metals*, in *Z. Phys. Chem.* **156** (1987).
- ¹³R. J. Highmore, J. E. Evetts, A. L. Greer, and R. E. Somekh, *Appl. Phys. Lett.* **50**, 566 (1987).
- ¹⁴M. Atzmon, J. D. Verhoeven, E. D. Gibson, and W. L. Johnson, *Appl. Phys. Lett.* **45**, 1052 (1984).
- ¹⁵K. L. Chopra, *Thin Film Phenomena* (Krieger, Malabar, FL, 1969).
- ¹⁶W. J. Meng, E. J. Cotts, and W. L. Johnson, in *Interfaces, Superlattices and Thin Films*, edited by J. D. Dow and I. K. Schuller, Materials Research Society Symposia Proceedings (Materials Research Society, Pittsburgh, PA, 1987), Vol. 77.
- ¹⁷K. H. Buschow, *J. Phys. F.* **14**, 593 (1984).
- ¹⁸Z. Altounian, Tu Guo-hua, and J. O. Strom-Olsen, *J. Appl. Phys.* **54**, 3111 (1983).
- ¹⁹F. H. M. Spit, J. W. Drijiver, and S. Radelaar, *Scripta Metall.* **14**, 1071 (1980).
- ²⁰A. R. Miedema, *Phillips Tech. Rev.* **36**, 217 (1976); P. I. Leoff, A. W. Weeber, and A. R. Miedema, *J. Less-Common Met.* **140**, 299 (1988).
- ²¹N. Saunders and A. P. Miodownik, *J. Mater. Sci.* **1**, 38 (1986).
- ²²A. Pasturel, C. Colinet, and K. H. J. Buschow, in *Rapidly Quenched Metals*, edited by S. Steeb and H. Warlimont (Elsevier Science Publishers, 1985).
- ²³U. Gösele and K. N. Tu, *J. Appl. Phys.* **53**, 3252 (1982).
- ²⁴B. E. Deal and A. S. Grove, *J. Appl. Phys.* **36**, 3770 (1965).
- ²⁵J. C. Barbour, *Phys. Rev. Lett.* **55**, 2872 (1985).
- ²⁶B. M. Clemens, *Phys. Rev. B* **33**, 7615 (1986).
- ²⁷Y. D. Dong, G. Gregan, and M. G. Scott, *J. Non-Cryst. Solids* **43**, 430 (1981).
- ²⁸H. E. Kissinger, *Anal. Chem.* **29**, 1702 (1957).
- ²⁹W. J. Meng, C. W. Nieh, and W. L. Johnson, *Appl. Phys. Lett.* **51**, 1693 (1987).
- ³⁰S. B. Newcomb and K. N. Tu, *Appl. Phys. Lett.* **48**, 1436 (1986).